AIMS Materials Science, 3(1): 137-148.
DOI: 10.3934/matersci.2016.1.137
Received: 25 November 2015
Accepted: 14 January 2016
Published: 18 January 2016

http://www.aimspress.com/journal/Materials

Review

Smart materials for energy storage in Li-ion batteries

Christian M Julien [1,*], Alain Mauger [2], Ashraf E Abdel-Ghany [3], Ahmed M Hashem [3], and Karim Zaghib [4]

[1] Sorbonne Universités, UPMC Univ. Paris6, PHENIX, UMR 8234, 4 place Jussieu, 75005 Paris, France
[2] Sorbonne Universités, UPMC Univ. Paris6, IMPMC, 4 place Jussieu, 75005 Paris, France
[3] National Research Centre, Inorganic Chemistry Department, 33 El Bohouth St., (former El Tahrir St.), Dokki-Giza 12622, Egypt
[4] Energy Storage and Conversion, Research Institute of Hydro-Québec, Varennes, Québec, J3X 1S1 Canada

* **Correspondence**: Email: Christian.Julien@upmc.fr.

Abstract: Advanced lithium-ion batteries contain smart materials having the function of insertion electrodes in the form of powders with specific and optimized electrochemical properties. Different classes can be considered: the surface modified active particles at either positive or negative electrodes, the nano-composite electrodes and the blended materials. In this paper, various systems are described, which illustrate the improvement of lithium-ion batteries in term of specific energy and power, thermal stability and life cycling.

Keywords: lithium-ion batteries; insertion electrodes; coatings; composites; blends

1. Introduction

Smart materials are designed as compounds exhibiting properties that can be significantly changed in a controlled fashion by external stimuli, such as electric field in the case of energy storage and conversion devices [1]. The reaction may exhibit itself as electricity production (batteries, supercapacitors), change in color (smart windows, electrochromics), catalytic effect, etc. Advanced lithium-ion batteries contain several smart materials having specific and complementary function such as insertion electrodes, i.e. cathode and anode, and separator [2].

Insertion compounds (ICs) have peculiar properties of mixed conduction for both electrons and ions, so that the redox reaction can be delocalized in their volume, the reason why they can be used as active materials of electrodes [3]. Their high capability to host foreign ions depends of several factors: structure, transport, particle shape, etc., so that the relationship between structure and electrochemical features has been evaluated with special attention. For materials currently used as positive electrode in lithium batteries, the different crystal chemistries are examined from the basic reaction driven by charge transfer from the guest Li^+ ions to the conduction band of the host compound. Thus electron-donating species can take place in a reversible reaction classically represented by the scheme**:**

$$x\mathrm{A}^+ + x\mathrm{e}^- + \langle \mathrm{H} \rangle \leftrightarrow [\mathrm{A}_x{}^+ \langle \mathrm{H} \rangle^{x-}], \quad (1)$$

in the usual case, where ⟨H⟩ is the host, A is an alkali metal, *x* the molar insertion fraction and $[\mathrm{A}_x{}^+\langle \mathrm{H} \rangle^{x-}]$ is the final product. The electronic transport plays an important role in such a reaction towards the formation of ICs. It also undergoes phase transitions as the change in the crystallographic parameters of the ⟨H⟩ structure has an electronic character. Consequently, one can consider various classes of insertion reaction that corresponds to the different steps in the electronic delocalization .The level of acceptance can be either a discrete atomic state, or a molecular level of a discrete polyatomic structural entity, or part of a conduction band. In this aspect, Fig. 1 shows the scheme of the insertion mechanism in a tunnel framework MnO_2 as positive electrode in lithium battery. During the discharge process, ions and electrons flow into the empty sites of the cathode placed between an ionic conductor and a current collector.

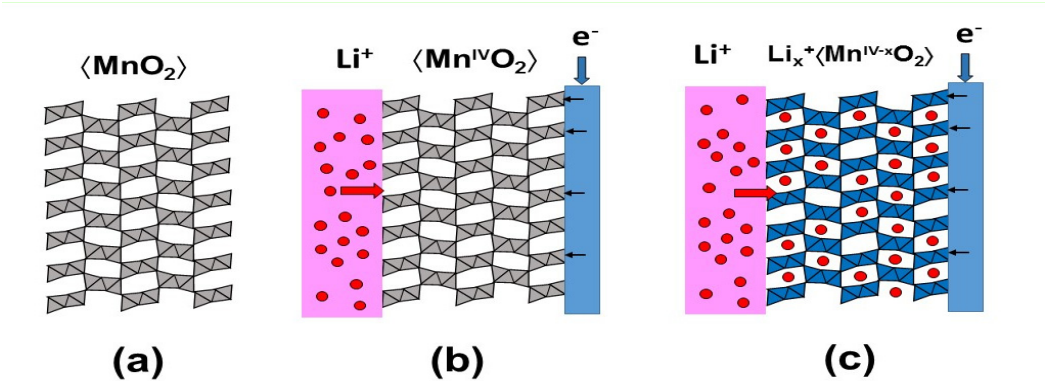

Figure 1. Scheme of the insertion mechanism. (a) The tunnel framework of the MnO_2 cathode material, (b) charge state of the $Mn^{IV}O_2$ electrode with empty sites and (c) partial discharge state for which manganese cations are in the (4-*x*) oxidation state.

In this paper, we describe some advanced "smart systems" having very sophisticated structures that were elaborated in the view of use as active materials for electrodes in high-power lithium batteries for electric vehicles (EVs). Such an application requests several advantages with regard to low cost, non-toxicity, environmental friendless and high safety associated with remarkable chemical and thermal stabilities and tolerance to overcharge and over-discharge. These smart systems include surface modified compounds, blended materials and nano-composites. The cathode materials such as $LiNi_{1/3}Mn_{1/3}Co_{1/3}O_2$ (NMC), $Li[Li_{0.1}Mn_{1.85}Al_{0.05}]O_4$ (LMA), $LiMn_2O_4$ (LMO),

$Li_{1.2}Ni_{0.13}Mn_{0.54}Co_{0.13}O_2$ (Li-rich NMC), $Li_{4/3}Mn_{5/3}O_4$, $LiFePO_4$ (LFP), $LiMnPO_4$ (LMP), and the anode material nano-$Li_4Ti_5O_{12}$ have been selected here, since these the best representatives of the progress that has been achieved these recent years.

2. Surface-Modified Positive Electrodes

A constant progress to improve the calendar and the cycling life of electrodes in Li-ion batteries without sacrificing the safety issues is obtained owing to the surface treatment of the electrode particles. Fabricating smart materials by the coating of particles with a thin layer (~ 2–3 nm) that protects the core region from side reactions with the electrolyte, i.e. formation of the solid-electrolyte interphase (SEI), prevents the loss of oxygen and the dissolution of the metal ions in the electrolyte, or simply improves the conductivity of the powder [4]. Figure 2 shows the realization of a phosphate coating onto NMC particle by a moderate heat treatment (T_a < 700 °C).

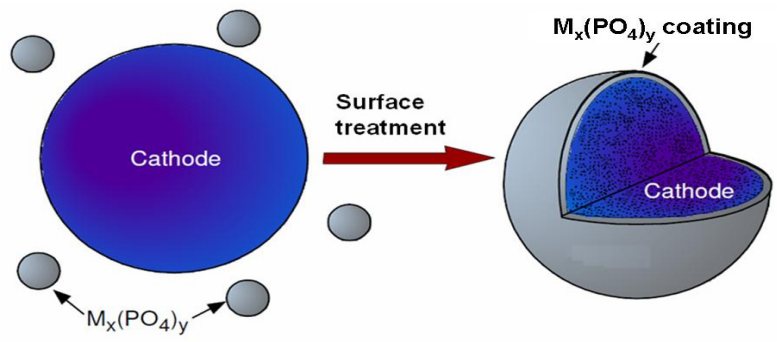

Figure 2. Scheme showing the preparation of NMC cathode particle coated by surface treatment.

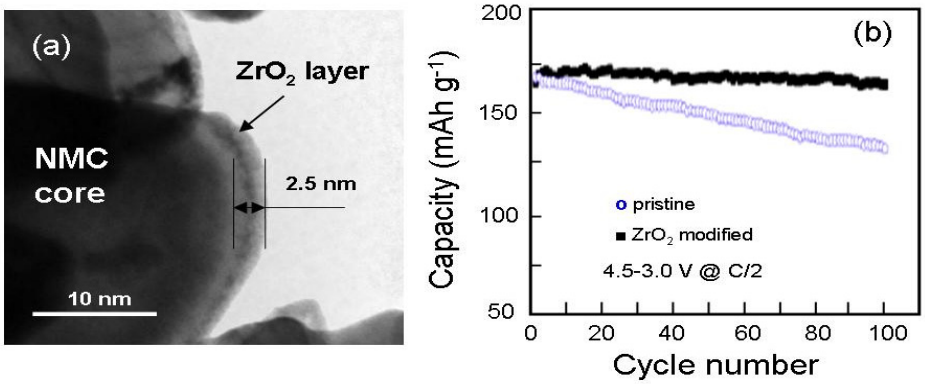

Figure 3. (a) TEM image of a ZrO_2-coated NMC particle [5]. Coating was obtained using $ZrO(NO_3)_2$ that was first dissolved in ethanol. (b) Discharge specific capacity of pristine and 1 wt.% zirconia-modified NMC cathode, with Li metal as counter-electrode. The cathodes were charged and discharged at C/2 rate in the 3.0–4.5 potential range.

The use of lithium transition-metal oxides such as NMC, which exhibit poor cycling stability, is limited because of the formation of a SEI at high cut-off voltage and thermal runaway at high rate.

Nevertheless, improvements can be achieved by fabricating a smart material with a special surface treatment (coating) that aims to protect the particles against the electrolyte. Various substances, Al-based oxides and phosphates, i.e. Al_2O_3, $AlPO_4$, and also ZrO_2 are widely used [4]. Among them, ZrO_2 is of particular interest as it exhibits a negative zeta potential, basic surface, and strong bonding, which are beneficial for trapping HF that is formed in $LiPF_6$ organic carbonate electrolytes, and maintaining the chemical stability. A 2.5-nm thick zirconia coating (Fig. 3a) is efficient for decreasing the irreversible capacity loss of NMC particles during the high potential cycling. Figure 3b shows the specific capacity for spherical shape particles (8 μm size) of pristine and 1 wt.% ZrO_2-modified NMC cathode obtained from $ZrO(NO_3)_2$ dissolved in ethanol [5]. The comparison between performance of uncoated and ZrO_2-coated NMC (Fig. 3b) shows that the surface modified electrode preserves a specific capacity of 170 mAh g^{-1} after 120 charge-discharge cycles.

Recently, a highly uniform coating layer has been obtained by sputtering zirconium oxide on LMC [6]. These authors have determined that the surface is coated with ZrO_2, while Zr^{2+} is detected below the surface layer, acting as a dopant. The overall process was then called ZrO_x-coating. Cycling testing was conducted by using the constant current followed by holding the constant voltage (4.5 V for 30 min) in the potential range of 3.0–4.5 V vs. Li^0/Li^+ ,and the C-rate was fixed at 1C (160 mA g^{-1}), except for the first 2 cycles (formation cycles, C-rate of C/4). The capacity was still stabilized at 150 mAh g^{-1} after 200 cycles.

$LiMn_2O_4$ (LMO) spinel is an attractive cathode element, mainly because its thermal stability is much better than that of the lamellar compounds such as $LiCoO_2$ [7]. However, it suffers from poor cycling behavior. The dissolution of manganese in the electrolyte is of major concern [8], since it reduces the calendar life of the battery. In addition, the kinetics of this reaction of LMO with the electrolyte increases with the temperature, so that LMO particles need a special treatment. To overcome the problem of poor cycling, it was suggested that both Li and Al doping in Mn sites of LMO spinel avoid Mn dissolution [9] and a surface-modified $Li[Li_{0.1}Mn_{1.85}Al_{0.05}]O_4$ (LMA) by bismuth oxyfluoride (BiOF) coating has improved electrochemical properties [10]. The advantage of fluoride is that it is stable in HF. Since BiOF is not electro-active, the coating decreases the capacity, but it increases very much the capacity retention at high temperature. Recently, results have been obtained with BiOF-coated LMA, since the irreversible capacity loss after 100 charge-discharge cycles is significantly reduced. Figure 4 presents the HRTEM images of pristine BiOF-coated spinel particles after 100 cycles. Comparable improvements have been observed by coating AlF_3 on $Li_{1.1}Al_{0.05}Mn_{1.85}O_4$ [11] and $LiMn_2O_4$ coated with 2.92 wt.% LaF_3 displays capacity [12].

Another route that has been used recently is coating $LiMn_2O_4$ with a carbon layer, typically 1.5 nm thick. The C-$LiMn_2O_4$ composite cathode maintains 97.76% of its initial discharge capacity after 100 charge–discharge cycles at C/10 rate, proving that the carbon layer avoiding the core material direct contact with the acidic electrolyte and suppression of Mn dissolution into electrolyte [13]. The current strategy to synthesize nanowires is to use self-support template, which is not suited at mass production. However, it is now possible to prepare carbon-coated $LiMn_2O_4$ nanowires without using a template [14]. The cathode prepared with C-$LiMn_2O_4$ nanowires adds the advantage of the nano-size of the wires, to obtain high-rate performance, and carbon protection to obtain long cycling life: Even after 1500 cycles at an extremely high current density of 30C, approximately 82% of its initial capacity can still be retained.

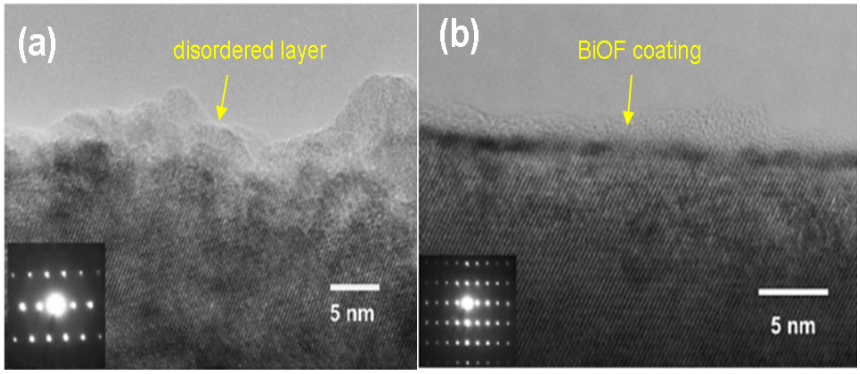

Figure 4. HRTEM images of $Li[Li_{0.1}Mn_{1.85}Al_{0.05}]O_4$ particles after 100 charge-discharge cycles [10]. Structural damage occurs on the surface the pristine spinel (a) while the surface of particle is well preserved with the BiOF-coating (b).

Carbon coated $LiFePO_4$ nanoparticles were used as surface coating agents for the 5-V electrode $LiMn_{1.5}Ni_{0.5}O_4$ spinel. A new mechano-fusion dry process was used, which provides a simple way to obtain surface coating for battery materials. Surface elemental analyses indicate that $LiFePO_4$ nanoparticles were not simply mixed with the $LiMn_{1.5}Ni_{0.5}O_4$, but successfully coated on its surface. This new composite was tested as a cathode for Li-ion batteries. $LiMn_{1.5}Ni_{0.5}O_4$ showed better capacity retention after $LiFePO_4$ coating, especially at high rate (>10C) as shown in Fig. 5. After 100 cycles at 1C, the capacity declined from 105 to 65 mAh g^{-1} for the bare $LiMn_{1.5}Ni_{0.5}O_4$. In contrast, 82 mAh g^{-1} of capacity was still obtained for the $LiFePO_4$-coated $LiMn_{1.5}Ni_{0.5}O_4$ with 75% of capacity retention after 140 cycles under 1C. The results suggest that the improved performance is due to the increasing of the surface conductivity due to the carbon coated $LiFePO_4$ covering, and the protection against reactions of $LiMn_{1.5}Ni_{0.5}O_4$ with the electrolyte [15].

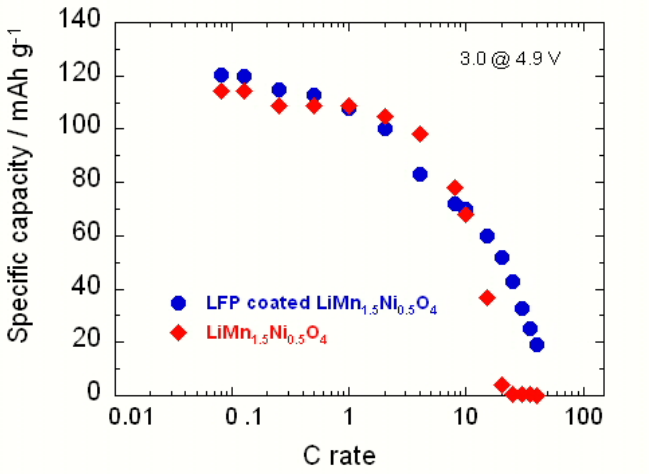

Figure 5. Discharge profiles of the Li//LFP-coated LMN cells at different C rates. The LFP coated was realized by mechano-fusion dry process [12].

3. Nano-Composite Electrode

To overcome the difficulty of carbon coating on $LiMnPO_4$ (LMP) olivine particles, it is possible to coat $LiMnPO_4$ with a thin layer of $LiFePO_4$ (10–20 nm) that takes benefit of the catalytic reaction of Fe with C, so that a 3 nm-thick layer of carbon can be deposited at the surface of this composite (Fig. 6) [16]. Using such a composite, the electrochemical properties of the carbon-coated LFP-LMP electrode are improved with respect to the carbon-coated $LiMn_{2/3}Fe_{1/3}PO_4$ solid solution with comparable Fe/Mn ratio (Fig. 7). Therefore, the use of a $LiFePO_4$ as a buffer layer between the high-density cathode element (like $LiMnPO_4$) and the carbon layer opens a new route to improve the performance of the olivine family as the active element of the cathode for Li-ion batteries. This result is attributable to the fact that the LFP shell allows for the coating of the composite, while it is difficult to deposit the carbon at the surface of LMP at temperature small enough to avoid its decomposition. This carbon layer improves the electrical contact between the particles, and consequently the performance at high C-rate. In addition, the LFP layer may avoid side reactions with the electrolyte, since the electrochemical properties do not degrade upon cycling, at least during the 100 first cycles that have been tested. The synthesis of composite particles of active elements of the olivine family is thus a promising route to improve the energy density of future Li-ion batteries, since both the LFP and the LMP are active materials, and the composite takes benefit of the higher redox potential of Mn^{2+}/Mn^{3+} vs. Li^0/Li^+.

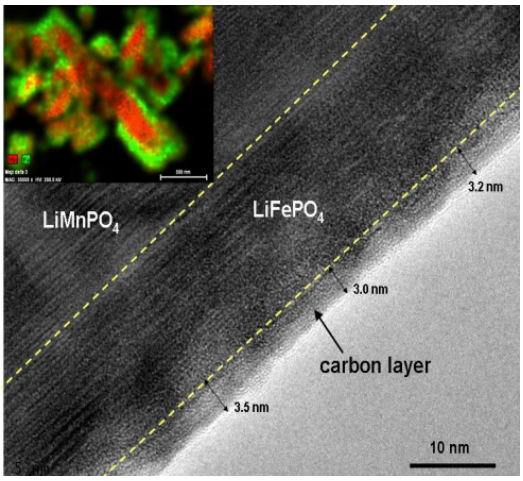

Figure 6. TEM image near the surface of LMP-LFP composite particle showing the different layers. Note the interface between $LiMnPO_4$ and $LiFePO_4$ is sharp and the carbon layer is continuous, but irregular, as a consequence of the rather low calcination temperature 600 °C. The typical EDX map of LMP (in red)-LFP (in green) particle is shown in the insert [16].

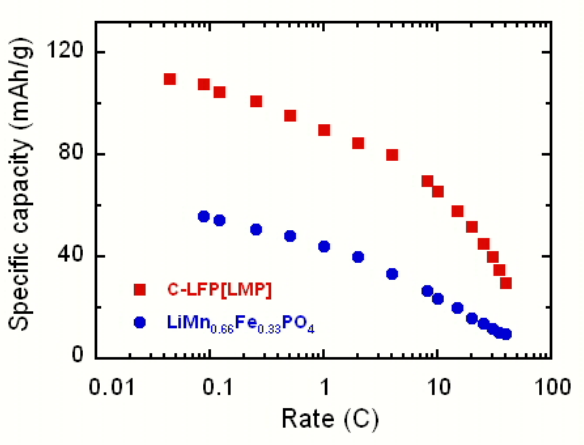

Figure 7. Modified Peukert plot of the C-$LiFePO_4$-$LiMnPO_4$ composite electrode compared with that of $LiMn_{2/3}Fe_{1/3}PO_4$ solid-solution material. Similar overall ratio of Mn over Fe and same size d = 300 nm of particles were used for comparison [16].

4. Blended Positive Electrodes

Blending electrodes is a new approach to design high-power battery for EVs [16,17]. The active material is formed by a mixture of two or more distinct lithium insertion compounds to achieve better balanced electrochemical performance than that of an individual compound (Fig. 8).

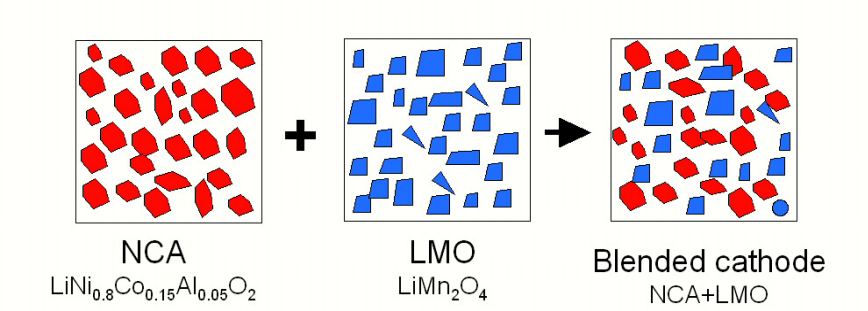

Figure 8. Scheme of a blended electrode composed by the layered $LiNi_{0.8}Co_{0.15}Al_{0.05}O_2$ and the spinel $LiMn_2O_4$.

The widely used NMC material as positive electrode delivers limited power at low state-of-charge (SOC) level due to the increased impedance, which is an inherent character of layered oxides. For example, the bended positive electrode (cathode) composed of Li-rich NMC ($Li_{1.2}Ni_{0.13}Mn_{0.54}Co_{0.13}O_2$) and $Li_{4/3}Mn_{5/3}O_4$ (LMO) spinel exhibits a higher specific capacity, i.e. 250 mAh g^{-1} than the spinel structure and lower irreversible capacity loss than Li-rich NMC but the average potential is inferior, i.e. 3–4 V vs. Li^0/Li^+ [7]. Another example is provided by the blended electrode $LiNi_{0.8}Co_{0.15}Al_{0.05}O_2$-$LiMn_2O_4$ (NCA-LMO) with the (1/3:2/3) stoichiometry [19], of which the electrochemical properties are presented in Fig. 9a-b. Illustrated by the Peukert plots (Fig. 9b), the improved performance of the NCA-LMO blend shows that specific capacity 140 mAh g^{-1} is maintained at high 10C rate.

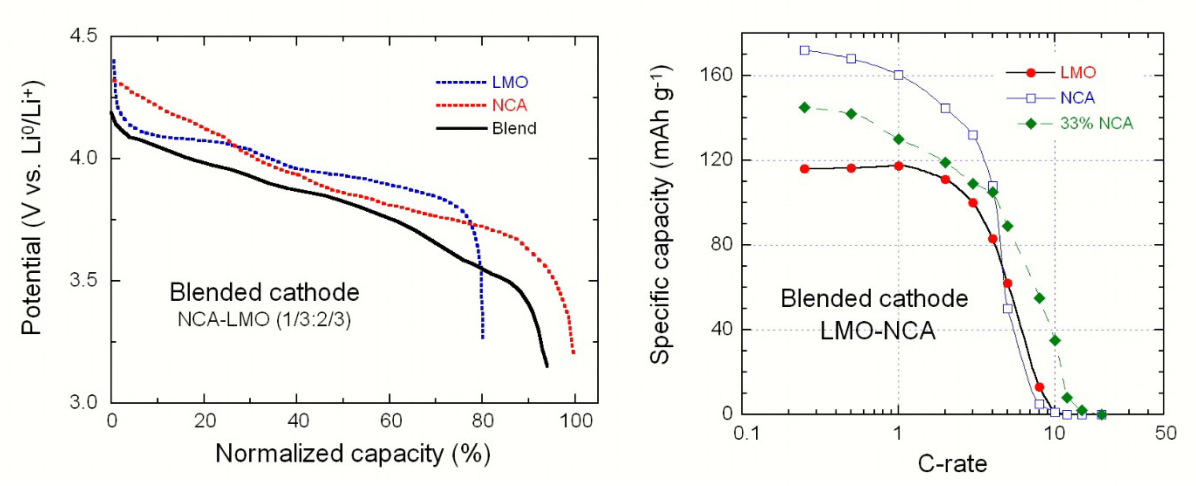

Figure 9. Electrochemical properties of the blended NCA-LMO electrode [19]. (a) Discharge curve of the blended electrode compared with those of components. (b) Peukert plot of the NCA-LMO compared with its single components.

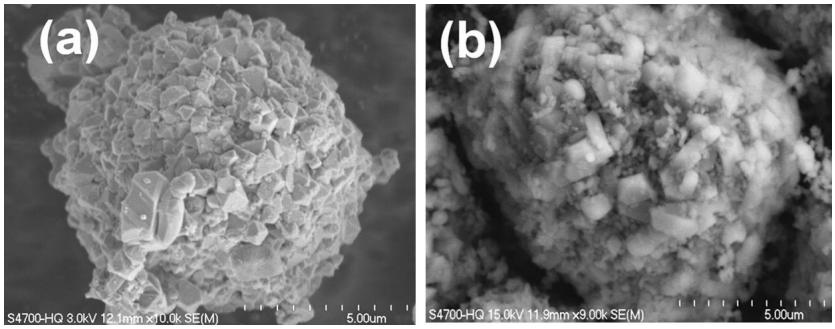

Figure 10. SEM picture of (a) the pristine NMC powder and (b) the NMC-LFP (70:30) blended electrode showing distinct compounds and the 3 wt.% carbon additive.

Another blended electrode is formed by the LFP-NMC system. LFP exhibits excellent rate capability by using nano-sized particles but delivers lower energy density than NMC, while NMC has a higher capacity, i.e. 180 mAh g^{-1} but its thermal stability is inferior that LFP [20]. Blended NMC-LFP electrode provides a good solution that achieves both energy and power capability. In the SEM image shown in Fig. 10, one discerns the two distinct components of which this blend is fabricated with the composition NMC-LFP (70:30). This blended material prepared by ultra microtomy has shown large NMC particles (several micrometers) and small LFP particles (<0.5 μm), but no LFP coating on MNC is observed. This could be due to the mechanical force applied during the microtomy. The Peukert plots of the NMC-LFP (70:30) blended electrode cycled at different cut-off voltages are shown in Fig. 11. These results indicate: (i) at low C-rate, the 4.8 V cut off provides the higher specific capacity of 180 mAh g^{-1} at C/10 rate but shows the lowest performance at high rates, (ii) higher capacity was obtained when the voltage cut-off is higher 4.1, 4.2 and 4.3 V, (iii) for the 4.1 V cut-off, the capacity fade less is pronounced, i.e. 0.12 mAh g^{-1} per cycle.

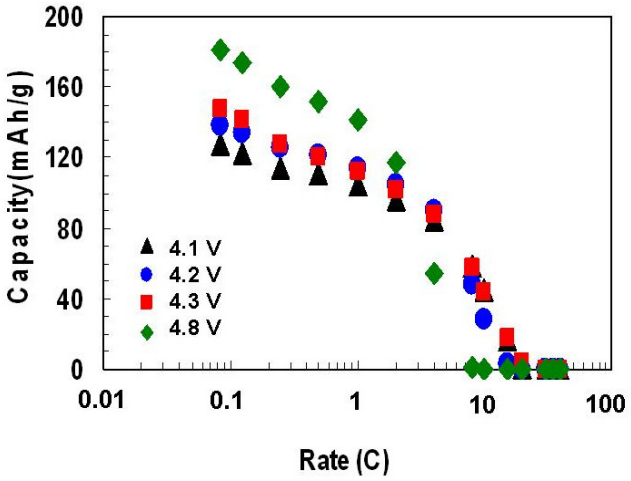

Figure 11. Specific capacity of the NMC-LFP (70:30) blended electrode as a function of C-rate in lithium cell cycled at different cut-off voltages.

5. Surface-Modified Negative Electrodes

The spinel $Li_4Ti_5O_{12}$ (LTO) is a zero-strain insertion compound, which exhibits excellent reversibility toward Li insertion/extraction [21]. On the other hand the high insertion potential (ca. 1.5 V vs. Li^0/Li^+) avoids the formation of the SEI and the reduction of the electrolyte. The preparation of a carbon-coated nanosized $Li_4Ti_5O_{12}$ nanoporous micro-sphere was made by a carbon pre-coating process combined with the spray drying method. The resulting sample delivers a reversible capacity of 160 mAh g^{-1} at C/5 rate, and shows remarkable rate capability by maintaining 79% of the capacity at 20 C (*vs.* C/5) [22]. Wang et al. [23] shown that rutile-TiO_2 as a carbon-free coating layer to improve the kinetics of LTO toward fast lithium insertion/extraction. The apparent chemical diffusion coefficient of Li^+ ions is found to be 4×10^{-13} cm^2s^{-1}, one order higher than pristine LTO. The preparation of LTO/carbon core-shell electrode was realized by using single-source carbon: metal acetate [24], single-walled carbon nanotubes [25], carbon black [26], solid-state reaction with pitch [27], among others.

Nano-sized LTO was synthesized by high-energy ball milling using TiO_2 anatase and Li_2CO_3 (molar ratio Li/Ti of 2.27) as the starting materials, to which carbon was added under the form of 3 wt.% vapor grown carbon fiber (VGC), plus 3 wt.% Denka-Black, Japan. The milling jar process was done in the presence of acetone used as liquid solvent [28]. The structure and morphology of LTO material are shown in Fig. 12. The milling process provides 90-nm sized particles with a homogeneous 1.5-nm thick carbon coating. Figure 13 shows the charge curves of C-$Li_4Ti_5O_{12}$/1 mol L^{-1} $LiPF_6$ in EC-DEC (1:1)/Li cells at different C-rates. Both the nanoporous morphology and highly conducting carbon coating layer in LTO particles gave rise to ultra-high rate capability (Fig. 13). The specific capacity is 166 mAh g^{-1} at C/24 rate and remains larger than 150 mAh g^{-1} at 30 C-rate. Such a negative electrode associated with a $LiFePO_4$ positive electrode was used in 18650-size cell that displays a discharge capacity of 130 mAh g^{-1} at low C-rate and retains more than 80 mAh g^{-1} at 40C rate [28].

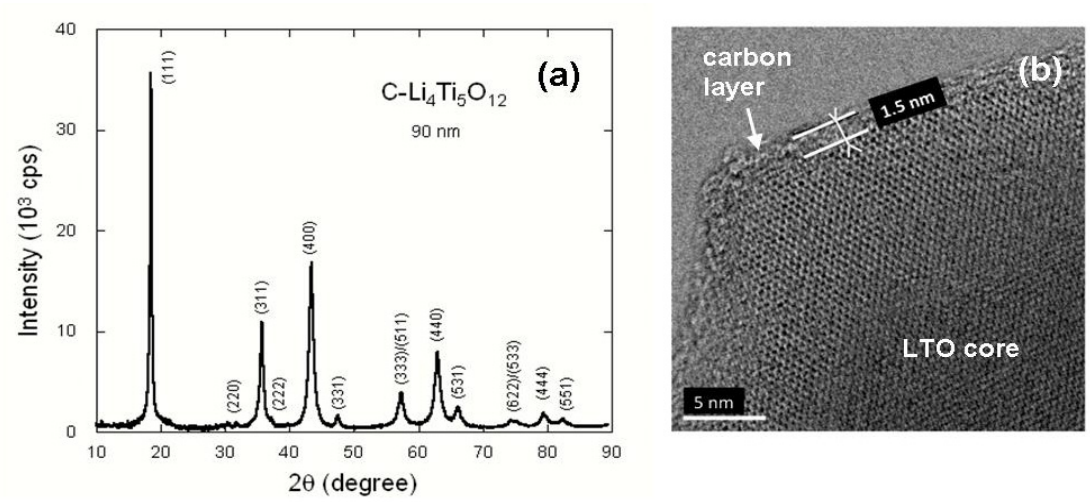

Figure 12. (a)X-ray diffractogram of carbon-coated LTO nano-particles (150 nm). (b) TEM image showing the carbon layer of the C-$Li_4Ti_5O_{12}$ composite.

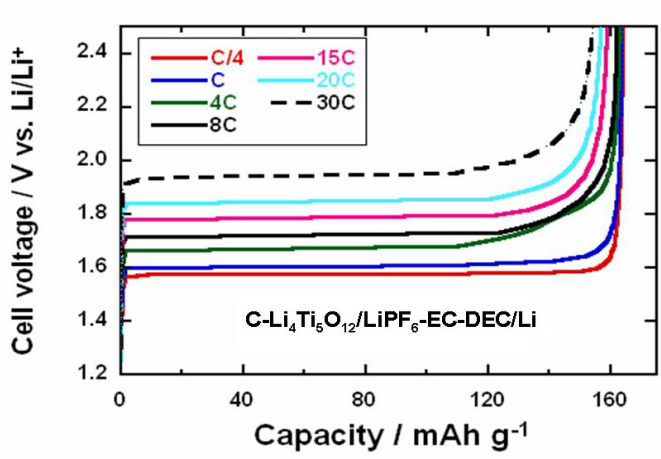

Figure 13. Charge curves of C-$Li_4Ti_5O_{12}$ /1 mol L^{-1} $LiPF_6$ in EC-DEC (1:1)/Li at different C-rates [28]. The electrode was deposited onto aluminum foil using 4 % water soluble binder plus thinner as bonder and 3 % VGCF, 3 % carbon as additive.

6. Conclusion

In this article, we have considered various smart materials used as electrodes in advanced Li-ion batteries. As this type of energy sources has become very promising to power electric vehicles and load-leveling applications, the development of new electrode materials requests update technology to provide electricity storage with long term stability. Advanced "smart systems" having very sophisticated structures were elaborated considering several advantages with regard to low cost, non-toxicity, environmental friendless and high safety associated with remarkable chemical and thermal stabilities and tolerance to overcharge and over-discharge. These smart systems include surface modification, blending and nano-composites. Cathode and anode materials such as

$LiNi_{1/3}Mn_{1/3}Co_{1/3}O_2$ (NMC), $Li[Li_{0.1}Mn_{1.85}Al_{0.05}]O_4$ (LMA), $LiNi_{0.8}Co_{0.15}Al_{0.05}O_2$ (NCA), $LiMn_2O_4$ (LMO), $LiFePO_4$ (LFP), $LiMnPO_4$ (LMP), and nano-$Li_4Ti_5O_{12}$ have been considered.

Conflict of Interest

There is no conflict of interest related to this document.

References

1. https://en.wikipedia.org/wiki/Smart_material (2015)
2. Julien CM, Mauger A, Vijh A, et al. (2015) *Lithium Batteries: Science and Technology*. Springer, New York.
3. Julien CM (2003) Lithium intercalated compounds, charge transfer and related properties. *Mater Sci Eng R* 40: 47–102.
4. Mauger A, Julien CM (2014) Surface modifications of electrode materials for lithium-ion batteries: status and trends. *Ionics* 20: 751–787.
5. Hashem AMA, Abdel-Ghany AE, Eid AE, et al. (2011) Study of the surface modification of $LiNi_{1/3}Co_{1/3}Mn_{1/3}O_2$ cathode materials for lithium-ion battery. *J Power Sources* 196: 8632–8637.
6. Lee JH, Kim JW, Kang HY, et al. (2015) The effect of energetically coated ZrO_x on enhanced electrochemical performances of $Li(Ni_{1/3}Co_{1/3}Mn_{1/3})O_2$ cathodes using modified radio frequency (RF) sputtering. *J Mater Chem A* 3: 12982–12991.
7. Thackeray MM, Johnson PJ, de Picciotto LA, et al. (1984) Lithium extraction from $LiMn_2O_4$. *Mater Res Bull* 19:179–187.
8. Amatucci GG, Schmutz CN, Blyr A, et al. (1997) Materials effects on the elevated and room temperature performance of C-$LiMn_2O_4$ Li-ion batteries. *J Power Sources* 69: 11–25.
9. Komaba S, Kumagai N, Sasaki T, et al. (2001) Manganese dissolution from lithium doped Li-Mn-O spinel cathode materials into electrolyte solution. *Electrochemistry* 69: 784–787.
10. Lee KS, Myung ST, Amine K, et al. (2009) Dual functioned BiOF-coated $Li[Li_{0.1}Al_{0.05}Mn_{1.85}]O_4$ for lithium batteries. *J Mater Chem* 19: 1995–2005.
11. Lee DJ, Lee KS, Myung ST, et al. (2011) Improvement of electrochemical properties of $Li_{1.1}Al_{0.05}Mn_{1.85}O_4$ achieved by an AlF_3 coating. *J Power Sources* 196: 1353–1357.
12. Chen Q, Wang Y, Zhang T, et al. (2012) Electrochemical performance of LaF_3-coated $LiMn_2O_4$ cathode materials for lithium ion batteries. *Electrochim Acta* 83: 65–72.
13. Jiang Q, Wang X, Tang Z (2015) Improving the electrochemical performance of $LiMn_2O_4$ by amorphous carbon coating. *Fullerenes, Nanotubes and Carbon Nano* 23: 676–679.
14. Sun W, Liu H, Bai G, et al. (2015) A general strategy to construct uniform carbon-coated spinel $LiMn_2O_4$ nanowires for ultrafast rechargeable lithium-ion batteries with a long cycle life. *Nanoscale* 7: 13173–13180.
15. Liu D, Trottier J, Charest P, et al. (2012) Effect of nano$LiFePO_4$ coating on $LiMn_{1.5}Ni_{0.5}O_4$ 5-V cathode for lithium ion batteries. *J Power Sources* 204: 127–132.
16. Zaghib K, Trudeau M, Guerfi A, et al. (2012) New advanced cathode material: $LiMnPO_4$ encapsulated with $LiFePO_4$. *J Power Sources* 204: 177–181.
17. Chikkannanavar SB, Bernardi DM, Liu L (2014) A review of blended cathode materials for use in Li-ion batteries. *J Power Sources* 248: 91–100.

18. Gao J, Manthiram A (2009) Eliminating the irreversible capacity loss of high capacity layered $Li[Li_{0.2}Ni_{0.13}Mn_{0.54}Co_{0.13}]O_2$ cathode by blending with other lithium insertion hosts. *J Power Sources* 191: 644–647.
19. Tran HY, Täubert C, Fleischhammer M, et al. (2011) $LiMn_2O_4$ spinel/$LiNi_{0.8}Co_{0.15}Al_{0.05}O_{0.2}$ blends as cathode materials for lithium-ion batteries. *J Electrochem Soc* 158: A556–A561.
20. Luo W, Li X, Dahn JR (2010) Synthesis, characterization and thermal stability of $Li[Ni_{1/3}Mn_{1/3}Co_{1/3-z}(MnMg)_{z/2}]O_2$. *Chem Mate*r 22: 5065–5073.
21. Ohzuku T, Ueda A, Yamamoto N (1995) Zero-strain insertion material of $Li[Li_{1/3}Ti_{5/3}]O_4$ for rechargeable lithium cells. *J Electrochem Soc* 142: 1431–1435.
22. Zhu GN, Liu HJ, Zhuang JH, et al. (2011) Carbon-coated nano-sized $Li_4Ti_5O_{12}$ Yong-Gang nanoporous micro-sphere as anode material for high-rate lithium-ion batteries. *Energy Environ Sci* 4: 4016–4022.
23. Wang YQ, Gu L, Guo YG, et al. (2012) Rutile-TiO_2 nano-coating for a high-rate $Li_4Ti_5O_{12}$ anode of a lithium-ion battery. *J Am Chem Soc* 134: 7874–7879.
24. Shen L, Li H, Uchaker E, et al. (2012) General strategy for designing core−shell nanostructured materials for high-power lithium ion batteries. *Nano Lett* 12: 5673–5678.
25. Choi JH, Ryu WH, Park K, et al. (2014) Multi-layer electrode with nano-$Li_4Ti_5O_{12}$ aggregates sandwiched between carbon nanotube and graphene networks for high power Li-ion batteries. *Sci Rep* 4: 7334.
26. Zaghib K, Dontigny M, Guerfi A, et al. (2012) An improved high-power battery with increased thermal operating range: C-$LiFePO_4$//C-$Li_4Ti_5O_{12}$. *J Power Sources* 216: 192–200.
27. Jung HG, Myung ST, Yoon CS, et al. (2011) Microscale spherical carbon-coated $Li_4Ti_5O_{12}$ as ultra-high power anode material for lithium batteries. *Energy Environ Sci* 4: 1345–1351.
28. Zaghib K, Dontigny M, Guerfi A, et al. (2012) An improved high-power battery with increased thermal operating range: C-$LiFePO_4$//C-$Li_4Ti_5O_{12}$. *J Power Sources* 216: 192–200.

AIMS Press

© 2016 Christian M Julien, et al., licensee AIMS Press. This is an open access article distributed under the terms of the Creative Commons Attribution License (http://creativecommons.org/licenses/by/4.0)